

# Interpretation of in-phase and out-of-phase BWR oscillations using an extended reduced order model and semi-analytical bifurcation analysis

Abdelhamid Dokhane<sup>a,b,\*</sup>, Dieter Hennig<sup>a,1</sup>, Rizwan-uddin<sup>c</sup>, Rakesh Chawla<sup>a,b</sup>

<sup>a</sup> Laboratory for Reactor Physics and Systems Behavior, Paul Scherrer Institute, CH-5232 Villigen, Switzerland

<sup>b</sup> Ecole Polytechnique Fédérale de Lausanne (EPFL) PHB-Ecublens, CH-1015 Lausanne, Switzerland

<sup>c</sup> Department of Nuclear, Plasma, and Radiological Engineering, University of Illinois, 103 S. Goodwin Avenue, Urbana, IL 61801, USA

Received 7 June 2006; accepted 12 December 2006

Available online 6 March 2007

## Abstract

An extended reduced order model is presented and applied to analyze global and regional oscillations in BWRs. Stability and semi-analytical bifurcation analyses are performed using this model in conjunction with the bifurcation code BIFDD to determine the stability limits for both in-phase and out-of-phase oscillation modes and the nature of Poincaré–Andronov–Hopf bifurcation. The results obtained show that both sub- and supercritical PAH bifurcations are encountered in different regions of the parameter space.

An in-depth investigation of the properties of the elements of the eigenvectors associated with these two modes of oscillation is carried out. Results show that these eigenvectors provide information as regards the corresponding oscillation mode (in-phase or out-of-phase) without solving the set of system ODEs. The analysis clearly brings out the fact that in-phase and out-of-phase oscillations are whole-system mechanisms. A clear distinction is thereby made between these oscillation modes, on the one hand, and the fundamental and first azimuthal neutronics modes on the other hand.

© 2007 Published by Elsevier Ltd.

## 1. Introduction

### 1.1. Motivation and scope of the present research

Two kinds of power oscillations have been observed in BWRs: in-phase oscillations, where neutron flux oscillations are in-phase at all the fuel bundles in the core, and regional or out-of-phase oscillations, where neutron flux one half of the core oscillates out-of-phase with respect to that of the other half. Because of the strong coupling between the neutronics and the thermal-hydraulics via the void and Doppler feedback reactivities, BWR instabilities

are also called nuclear-coupled-thermal-hydraulic instabilities.

In the context of nonlinear system analysis, an isolated periodic solution of the set of equations (self-sustained oscillations, also termed a limit cycle) can bifurcate under variation of one or more system parameter(s). The investigation of such system behavior is the principal objective of nonlinear stability and bifurcation analysis. So far, Poincaré–Andronov–Hopf (PAH) bifurcation is the main type of bifurcation that has been encountered during BWR bifurcation analysis.

Stability analysis of BWRs is usually carried out using large system codes (e.g. RAMONA (Wulf et al., 1984)) that simulate the nuclear power plant behavior with a high degree of modeling detail (Hennig, 1999). Because of the large computational effort required, system codes cannot in practice be employed for a detailed investigation of the complete manifold of solutions of the set of nonlinear

\* Corresponding author. Present address: King Saud University, College of Science, Department of Physics and Astronomy, P.O. Box 2455, Riyadh 11451, SA. Tel.: +966 14676626.

E-mail address: [adokhane@ksu.edu.sa](mailto:adokhane@ksu.edu.sa) (A. Dokhane).

<sup>1</sup> Present address: Heckelberger Ring 4, D-13055 Berlin, Germany.



rod dynamics, and a homogeneous equilibrium model (HEM) for the thermal-hydraulic treatment of the two-phase flow, the latter being based on the assumption that the single-phase enthalpy and two-phase quality have time-dependent spatially quadratic profiles.

The current, new nonlinear model has been developed by essentially extending the neutron kinetics and the thermal-hydraulic parts of the Karve model. For the neutron kinetics, we use  $\lambda$ -modes instead of  $\omega$ -modes mainly because the former approach allows easier validation via comparisons with codes that perform higher-mode neutron flux and feedback reactivity calculations. More importantly a model based on a drift flux representation (DFM) has been implemented instead of the HEM to represent the two-phase flow. Such a model is more appropriate since it takes into account: (a) the difference between the two-phase velocities (which is particularly important in low-flow regimes), and (b) the radially non-uniform void distribution inside the channel.

Benefiting from the developments in nonlinear dynamics theory, significant advances have been made in the stability analysis of BWRs using ROMs. Recent efforts have concentrated on bifurcation analyses in which the effects of different design and operational parameters on the bifurcation characteristics are analysed. Such analyses give important information that should be taken into account in the design and operational analysis of the next generation of nuclear reactors. As mentioned earlier, PAH bifurcations represent the main type of bifurcation that has been encountered during nonlinear BWR stability analyses using ROMs. A supercritical PAH bifurcation implies existence of stable periodic solutions close to the stability boundary (SB) in the linearly unstable region, while a subcritical PAH bifurcation implies unstable periodic solutions close to the SB in the linearly stable region.

The bifurcation analyses reported by March-Leuba et al. (1986a,b), Muñoz-Cobo et al. (1996, 2000), Karve et al. (1997) were purely numerical, i.e. only direct numerical integrations were performed. Purely analytical bifurcation analysis was first carried out by Muñoz-Cobo and Verdú (1991) using the March-Leuba et al. model (1986a,1986b). However, such analysis needs extensive mathematical manipulation and becomes almost impossible to carry out for higher order models. Moreover, this type of bifurcation analysis can be carried out only for one specific bifurcation parameter at a time, and must be repeated if the impact of different parameters is to be studied. On the other hand, numerical bifurcation can only be performed for a limited number of operational points. As a consequence of the limitations of these two approaches, the scope of these previous analyses was restricted to a small region of the rather large parameter space, in spite of the simplicity of the models used.

In the present research, an alternative approach to the above two has been adopted, in which analytical reduction of the Poincaré normal form via the center manifold theorem is carried out numerically (Hassard et al., 1981). This

approach, called semi-analytical bifurcation analysis, allows accurate and efficient evaluation of the entire parameter space of interest. It was Tsuji et al. (1993) who, in conjunction with a simple BWR model, first used a computer code called BIFOR2 and showed that the bifurcation, under certain conditions, is subcritical. Later, the same approach was used by van Bragt et al. (1999) in the framework of a natural circulation BWR model, by Rizwan-uddin (2000) using the simple March-Leuba model (1986a,1986b), by Zhou and Rizwan-uddin (2002) using the Karve model (1998), and by Dokhane et al. (2005), using the current thermal-hydraulic sub-model, in the framework of a heated channel model study. However, these studies used the bifurcation code BIFDD, a successor to BIFOR2 code, both developed by Hassard (1987), to carry out the semi-analytical bifurcation analysis. As indicated earlier, the BWR reduced order model developed currently is used to carry out semi-analytical bifurcation analysis, the BIFDD code being employed once again for the purpose. The resulting, more detailed phenomenological treatment provides deeper insight into the mechanisms behind BWRs instabilities and gives more realistic information on the solution types that may exist.

In the present research, an alternative approach to the above two has been adopted, in which analytical reduction of the Poincaré normal form via the center manifold theorem is carried out numerically (Hassard et al., 1981). This approach, called semi-analytical bifurcation analysis, allows accurate and efficient evaluation of the entire parameter space of interest. It was Tsuji et al. (1993) who, in conjunction with a simple BWR model, first used a computer code called BIFOR2 and showed that the bifurcation, under certain conditions, is subcritical. Later, the same approach was used by van Bragt et al. (1999) in the framework of a natural circulation BWR model, by Rizwan-uddin (2000) using the simple March-Leuba model (1986a,1986b), by Zhou and Rizwan-uddin (2002) using the Karve model (1998), and by Dokhane et al. (2005), using the current thermal-hydraulic sub-model, in the framework of a heated channel model study. However, these studies used the bifurcation code BIFDD, a successor to BIFOR2 code, both developed by Hassard (1987), to carry out the semi-analytical bifurcation analysis. As indicated earlier, the BWR reduced order model developed currently is used to carry out semi-analytical bifurcation analysis, the BIFDD code being employed once again for the purpose. The resulting, more detailed phenomenological treatment provides deeper insight into the mechanisms behind BWRs instabilities and gives more realistic information on the solution types that may exist.

The present paper is organized as follows. In Section 2, the ordinary differential equations (ODEs) of the different components of the developed BWR reduced order model, i.e. neutron kinetics, fuel heat conduction, and the thermal-hydraulic, are presented briefly. Section 3 is devoted to the validation of the thermal-hydraulic part of the model against experimental data and the comparison with several

other analytical models developed earlier for simulating thermal-hydraulic instabilities. In Section 4, semi-analytical bifurcation analysis is carried out with an in-depth investigation of the properties of the eigenvectors associated with the two oscillations modes. Furthermore, numerical simulations are carried out at certain operating points to validate the findings of the bifurcation analyses. Finally, a summary and conclusions of the present study are presented in Section 5.

## 2. Current reduced order model

The new reduced order model for nonlinear analysis developed currently includes all significant physical processes determining the dynamics of a BWR core. The strategy followed in the model development is the following: firstly, to develop a model as simple as possible from the mathematical point of view (simple geometry; ordinary, instead of partial differential equations (PDEs)) while preserving the most important physical phenomena; secondly, to have a model as close as possible to the system code RAMONA in order to allow a systematic comparison of the performance of the reduced order model with RAMONA (Dokhane et al., 2007). For the latter purpose, several of the correlations and assumptions in RAMONA have been used in the ROM. The current model comprises three main parts: spatial lambda-mode neutron kinetics with the fundamental and first azimuthal modes, fuel heat conduction dynamics, and core thermal-hydraulics based on a drift flux model representation of the two-phase flow. The recirculation loop has been replaced throughout this study by a constant total pressure drop boundary condition across the reactor core. This assumption is found to be acceptable for out-of-phase instabilities in general, and for small amplitudes in the case of in-phase oscillations (Dokhane, 2004).

It should be noted, as mentioned earlier, that this model is effectively an extension of the Karve model (Karve, 1998), in which we use a drift flux model instead of the homogenous equilibrium model for two-phase flow, and  $\lambda$ -modes instead of the  $\omega$ -modes for the neutron kinetics. Thus, the novel aspects are essentially: (i) the use of a DFM that includes the effects of both the drift velocity and the radially non-uniform void distribution inside the channel; and (ii) the feedback reactivity calculation methodology based on RAMONA estimation (Dokhane, 2004).

### 2.1. Neutron kinetics

The present neutron kinetics model is derived from two-energy group diffusion equations. It is based on the assumption that the neutron flux is expanded in terms of  $\lambda$ -modes. An important advantage in this context is the possibility to assess the accuracy of a simplified modelling (of reactivity feedback effects, etc.) via comparisons with the results of detailed system codes based on the  $\lambda$ -modes approach (Dokhane, 2004).

With the above assumptions, the modal kinetics equations for the fundamental and first azimuthal neutronics modes ( $n_0(t)$  and  $n_1(t)$ ), with the two corresponding delayed neutrons precursors ( $U_0(t)$  and  $U_1(t)$ ), are (Muñoz-Cobo et al., 1996; Dokhane, 2004)

$$\frac{dn_0(t)}{dt} = \frac{1}{A_0} [(\rho_{00}(t) - \beta)n_0(t) + \rho_{01}(t)n_1(t)] + \lambda U_0(t) \quad (1)$$

$$\frac{dn_1(t)}{dt} = \frac{1}{A_0} [\rho_{10}(t)n_0(t) + (\rho_{11}(t) + \rho_1^s - \beta)n_1(t)] + \lambda U_1(t) \quad (2)$$

$$\frac{dU_0(t)}{dt} = \frac{\beta}{A_0} n_0(t) - \lambda U_0(t) \quad (3)$$

$$\frac{dU_1(t)}{dt} = \frac{\beta}{A_0} n_1(t) - \lambda U_1(t) \quad (4)$$

where  $\rho_{mn}(t)$  is the total feedback reactivity for the coupling between the  $m$ th-mode and the  $n$ th-mode. The governing neutron kinetics equations are coupled with the equations of the heat conduction and the thermal-hydraulic via the feedback reactivity terms. In this model, the void and Doppler feedback reactivities are considered to be the only relevant feedback mechanism.

The models for the void and Doppler feedback reactivities are described in Dokhane (2004). They are based on the assumption of linear reactivity profiles in terms of the void fraction and fuel temperature, respectively, as follows:

$$\rho_{mn}(t) = \text{fact}_{mn} \cdot \sum_{l=1}^2 c_{1mn,l}(\alpha_l(t) - \alpha_{0,l}) + c_{2mn,l}(T_{\text{avg},l}(t) - T_{\text{avg},0,l}) \quad (5)$$

where the index  $l$  stands for the channel number.

As mentioned earlier, only two channels, each representing one half of the reactor core, are considered currently. The quantities  $\alpha_{0,l}$  and  $T_{\text{avg},0,l}$  are the reference steady-state void fraction and the average fuel temperature in the channel  $l$ , respectively. The quantities  $T_{\text{avg},l}(t)$  and  $T_{\text{avg},0,l}(t)$  are equivalent to  $T_{f,l}(t)$  and  $T_{f,0,l}(t)$  in Dokhane (2004), respectively. The terms  $c_{1mk,l}$  and  $c_{2mk,l}$  are the void and Doppler feedback reactivity coefficients, respectively. Finally, as discussed in Dokhane (2004),  $\text{fact}_{mn}$  is a feedback gain parameter, introduced as a multiplier of the corresponding feedback reactivity, in order to increase the feedback gain coupling between the first and fundamental modes and thus enable the excitation of out-of-phase oscillation phenomena in specific cases. It is also used as the bifurcation parameter.

### 2.2. Fuel rod heat conduction

The fuel rod is modelled separately in the two axial regions corresponding to the single and two-phase regions of the boiling channel. In each of these regions, it is modelled with three distinct radial regions, the fuel pellet ( $0 < r < r_p$ ), the gap ( $r_p < r < r_g$ ), and the clad ( $r_g < r < r_c$ ). The heat conduction model is based on the following assumptions:

- Azimuthal symmetry.
- Neglected heat conduction in the  $z$ -direction.
- Time-dependent, spatially uniform volumetric heat generation.

The fuel rod sub-model used here was originally developed and validated by Karve (1998). Because detailed derivation of this sub-model is available in Karve (1998) and Dokhane (2004), only the final ODEs are presented. In brief, for each channel, four ODEs are developed from the heat conduction PDE. These ODEs are for the two coefficients of each of the two spatially piecewise quadratic representations of the fuel pellet temperature in the single and two-phase regions of the channel. In an explicit index form, these ODEs can be written as

$$\frac{dT_{1,j\phi,l}(t)}{dt} = ll_{1,1,j\phi,l}T_{1,j\phi,l}(t) + ll_{2,1,j\phi,l}T_{2,j\phi,l}(t) + ll_{3,1,j\phi,l}[c_q(n_0(t) - \tilde{n}_0) + c_q\xi_1 n_1(t)] \quad (6)$$

$$\frac{dT_{2,j\phi,l}(t)}{dt} = ll_{1,2,j\phi,l}T_{1,j\phi,l}(t) + ll_{2,2,j\phi,l}T_{2,j\phi,l}(t) + ll_{3,2,j\phi,l}[c_q(n_0(t) - \tilde{n}_0) + c_q\xi_2 n_1(t)] \quad (7)$$

where  $j\phi$  stands for single ( $1\phi$ ) or two-phase ( $2\phi$ ) region, and  $l$  stands for channel number (1 or 2). The factors  $ll_{1,s}$ ,  $ll_{2,s}$ , and  $ll_{3,s}$  are somewhat complicated constants which depend on the design parameters (Dokhane, 2004).

### 2.3. Thermal-hydraulics

The heat generated in the fuel rod is conducted and convected to the coolant in the flow channel. The single-phase coolant enters the bottom of the channel with a velocity  $v_{\text{inlet}}(t)$  and temperature  $T_{\text{inlet}}$ , and then starts boiling at a certain level—called the boiling boundary  $\mu(t)$ —at which the coolant reaches the saturation temperature  $T_{\text{sat}}$ . Above the boiling boundary, the coolant is a mixture of two phases, i.e. water and steam. The flow channel is accordingly divided into two regions, the single-phase and two-phase regions.

The three-dimensional mass, energy, and momentum equations in the single-phase and two-phase regions, that describe the fluid mechanics in the channel, are averaged over the cross-section of the flow channel to arrive at equations that depend only on a single spatial variable (axial position  $z$ ) and time. Then, for each representative flow channel,<sup>2</sup> ODEs are developed from the one-dimensional time-dependent PDEs by carrying out symbolic integration using a weighted residual method in which spatial approximations for the single-phase enthalpy and two-phase quality are used (Karve, 1998).

The thermal-hydraulic model is based on the following three principal assumptions:

- A drift flux model is used to represent the two-phase flow, rather than a homogeneous equilibrium model; such a model is more appropriate since it takes into account (a) the difference between the two-phase velocities (the drift velocity  $V_{gj}$ ), particularly important in the case of low flow rates, and (b) the radially non-uniform void distribution (the void distribution parameter  $C_0$ ) inside the channel.
- The time-dependent single-phase enthalpy and two-phase quality have spatially quadratic profiles. These two assumptions have been successfully validated and used earlier (Karve, 1998) with the homogeneous equilibrium model for two-phase flow.
- Subcooled nucleate boiling has been ignored.

Since the thermal-hydraulic model has been described in detail in Dokhane (2004) and Dokhane et al. (2005), only the final ODEs are presented here. In brief, for each channel, five ODEs result from the integration of the one-dimensional time-dependent continuity, energy and momentum equations in the single and two-phase regions, using a weighted residuals procedure

$$\frac{da_1(t)}{dt} = \frac{6}{\mu(t)} [N_\rho N_r N_{\text{pch},1\phi}(t) - v_{\text{inlet}}(t)a_1(t)] - 2v_{\text{inlet}}(t)a_2(t) \quad (8)$$

$$\frac{da_2(t)}{dt} = \frac{6}{\mu^2(t)} [N_\rho N_r N_{\text{pch},1\phi}(t) - v_{\text{inlet}}(t)a_1(t)] \quad (9)$$

$$\frac{ds_1(t)}{dt} = \frac{1}{ff_5(t)} \left[ ff_1(t) \frac{d\mu(t)}{dt} + ff_2(t) \frac{dv_{\text{inlet}}(t)}{dt} + ff_3(t) \frac{dN_{\text{pch},2\phi}(t)}{dt} + ff_4(t) \right] \quad (10)$$

$$\frac{ds_2(t)}{dt} = \frac{1}{ff_{10}(t)} \left[ ff_6(t) \frac{d\mu(t)}{dt} + ff_7(t) \frac{dv_{\text{inlet}}(t)}{dt} + ff_8(t) \frac{dN_{\text{pch},2\phi}(t)}{dt} + ff_9(t) \right] \quad (11)$$

$$\frac{dv_{\text{inlet}}(t)}{dt} = \frac{1}{ff_{14}(t)} \left( ff_{11}(t) \frac{d\mu(t)}{dt} + ff_{12}(t) \frac{dN_{\text{pch},2\phi}}{dt} + ff_{13}(t) \right) \quad (12)$$

where  $a_1(t)$  and  $a_2(t)$  are the coefficients of the linear and quadratic terms for the liquid enthalpy profile,  $s_1(t)$  and  $s_2(t)$  are the coefficients of the linear and quadratic terms for the quality profile, and  $v_{\text{inlet}}(t)$  is the liquid velocity at the channel inlet. The expressions  $ff_n(t)$ ,  $n = 1, \dots, 14$  are complicated intermediate quantities, which depend on the phase variables, the operating parameters and the design parameters (Dokhane, 2004).

In summary, the dynamical system that results from the current two-channel reduced order model consists of 22 ODEs, four from the neutron kinetics model, ten that describe the thermal-hydraulic model (five for each channel), and eight ODEs for the fuel rod heat conduction (two equations for each phase, in each channel). The set of 22 ODEs can be written in a compact form as:

<sup>2</sup> Two channels have been considered in the present model.

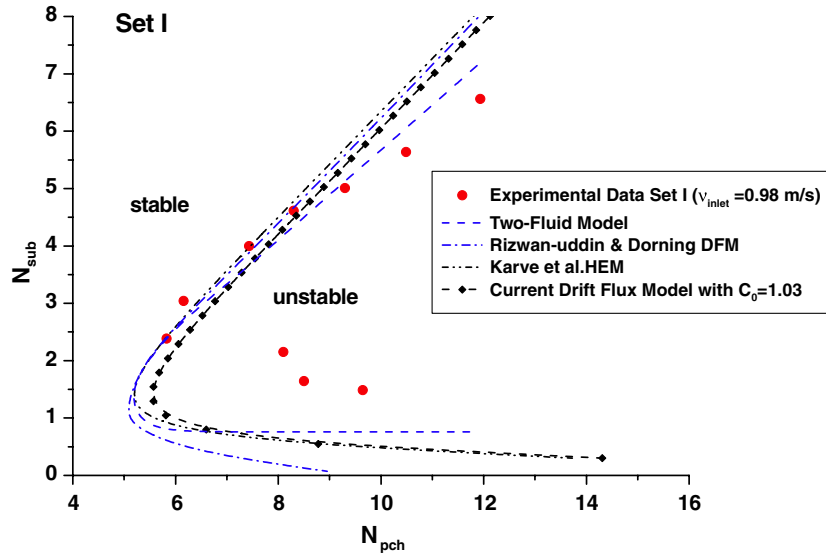


Fig. 1. Comparison of calculated stability boundaries with Set I experimental data ( $v_{\text{inlet}} = 0.98$  m/s).

$$\dot{X}(t) = F(X; \kappa) \quad (13)$$

where  $X(t)$  is the vector of 22 phase variables and  $\kappa$  is the vector of parameters that includes both the operating and design parameters

$$\kappa = (N_{\rho}, N_r, N_{\text{pch},1\phi}, N_{\text{pch},2\phi}, K_{\text{inlet}}, K_{\text{exit}}, N_{f,1\phi}, N_{f,2\phi}, Fr, C_0, V_{gj}) \quad (14)$$

Typical numerical values for the design and operating parameters of a General Electric Company (GE) BWR-6, with an approximate power of 1100 MWe, have been used in the present context (Dokhane, 2004).

### 3. Validation of the thermal-hydraulic part of the model

Since the phenomenon of thermally induced two-phase flow instability is of basic interest for the design and operation of BWRs, the aim in this section is to validate the current thermal-hydraulic model against appropriate experimental data and to compare its performance with the results obtained using several earlier models that were developed to simulate density wave oscillations.

Saha et al. (1976) carried out an experimental study on the onset of self-sustained thermal-hydraulic two-phase density wave oscillations. The experimental facility used consists of a uniformly heated boiling channel with Freon-113 as the operating fluid. Fig. 1 shows a simplified schematic sketch of this facility. The experimental data sets were generated by changing the inlet velocity  $v_{\text{inlet}}$ . For each experiment, the system pressure, the inlet and exit restrictions, and the inlet velocity ( $v_{\text{inlet}}$ ) were kept constant. The inlet subcooling was established by adjusting the preheating system, and the power was then increased in small steps until sustained flow oscillations were observed, thus identifying points on the stability boundary. Consequently, such points were plotted on the subcooling number ( $N_{\text{sub}}$ ) versus the equilibrium-phase-change num-

Table 1

Operating conditions for Sets I, III, V and VI of the Saha et al. experiments (Saha et al., 1976)

	Set I	Set III	Set V	Set VI
Pressure (bar)	12.1	10.3	12.1	12.1
$v_{\text{inlet}}$ (m/s)	0.98	1.02	0.72	1.49
$K_{\text{inlet}}$	2.85	2.85	6.55	6.55
$K_{\text{exit}}$	2.03	2.03	2.03	2.03

ber ( $N_{\text{pch}}$ ) plane. The operating conditions for different sets of experiments are given in Table 1.

It should be emphasized that, although these experiments were performed for a heated channel, they are very relevant to BWR stability analysis since the thermal-hydraulic phenomena investigated are of paramount importance in this context. Figs. 1 and 2 show the comparison of the stability boundaries calculated using the thermal-hydraulic model<sup>3</sup> with the experimental data (Sets I and VI) as re-evaluated by Rizwan-uddin and Dorning (1985).<sup>4</sup> Also compared in the figures are the stability boundaries calculated using several models that were developed earlier to study two-phase flow instabilities. These models are: (i) the two-fluid (Eq. (6)) model developed by Dykhuizen et al. (1986) that, naturally, includes subcooled boiling, (ii) the non-equilibrium slip model of Saha and Zuber (1978) that also includes subcooled boiling, but with a flat void profile ( $C_0 = 1$ ), (iii) the Ishii and Zuber slip

<sup>3</sup> In this study, all the points on a SB have the same coolant inlet velocity value. The SB is generated using the code BIFDD in which a system parameter, say  $N_{\text{sub}}$ , is chosen which can be incremented in small steps, then a second parameter, say  $N_{\text{pch}}$ , is selected. The second parameter is varied until it reach a critical value that corresponds to a point on the SB.

<sup>4</sup> Rizwan-uddin and Dorning found some errors in the evaluation of the dimensionless numbers  $N_{\text{sub}}$  and  $N_{\text{pch}}$  for the experimental data. These resulted from errors in the thermodynamic properties that were used to calculate the dimensionless numbers (Rizwan-uddin and Dorning, 1986).

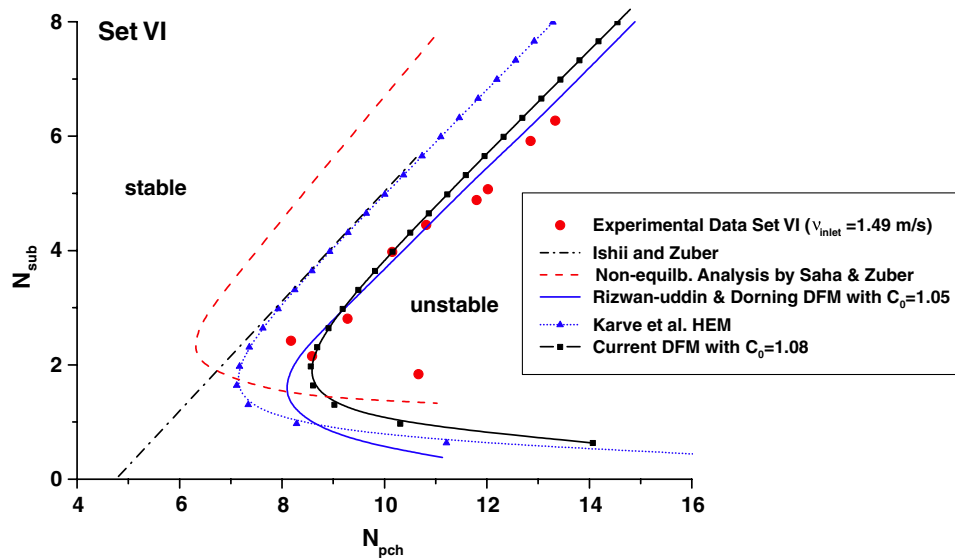


Fig. 2. Comparison of calculated stability boundaries with Set VI experimental data ( $v_{\text{inlet}} = 1.49$  m/s).

model (1970) based on a simplified stability criterion with a flat void profile, (iv) the drift flux model developed by Rizwan-uddin and Dorning (1986), and (v) the homogeneous equilibrium model of Karve (1998).

Fig. 2 shows the current model benchmarked against the experimental data for Set I with  $v_{\text{inlet}} = 0.98$  m/s, as well as against the two-fluid model, the Rizwan-uddin and Dorning DFM, and the Karve HEM. For large values of the inlet subcooling, all models are in good agreement with the experimental data. For lower values of  $N_{\text{sub}}$ , the differences between the models, however, are very small compared to the deviation between the models and the experimental results.

The importance of a radially non-uniform void distribution is clearly shown in Fig. 3 for the Set VI experimental data with  $v_{\text{inlet}} = 1.49$  m/s. It should be emphasized that this value of inlet velocity is in the range of values representative of an actual BWR,<sup>5</sup> so that these data are particularly relevant as validation base. The SBs predicted by the current model ( $C_0 = 1.08$ ) and the Rizwan-uddin and Dorning model ( $C_0 = 1.05$ ) are seen to agree very well with the experimental data. This is because for large values of  $V_{\text{inlet}}$ ,  $C_0$  is larger than 1 and, therefore, the models based on  $C_0 = 1$  (HEM or slip models) are likely to be inadequate. For lower values of  $N_{\text{sub}}$ , the Saha and Zuber model fits the data best, followed by the current model. It should be pointed out that, although the current model and the Rizwan-uddin and Dorning model are based on the same drift flux approach, they are constructed differently. The Rizwan-uddin and Dorning model is an exact model, *i.e.*, involves a direct integration of the first order, nonlinear, functional, ordinary differential equations. However, the authors ignored the higher order terms in a small parameter proportional to  $(C_0 - 1)$ . The present DFM is based on

two assumptions implying an approximate spatial treatment, *viz.* that the single-phase enthalpy and the two-phase quality have a quadratic dependence on the spatial  $z$  direction. Higher order terms, such as that of  $(C_0 - 1)$ , however, have not been neglected. This could explain why the current model fits the data better than the Rizwan-uddin and Dorning model for low values of  $N_{\text{sub}}$ .

To summarize, the current thermal-hydraulic model has been found to be in good agreement with the Saha *et al.* experimental data for large  $N_{\text{sub}}$ , as is the case for several, earlier developed models. For lower values of  $N_{\text{sub}}$ , the current model results compare with the experiment as well as the existing models, so that its validation against the experimental data can be considered to be globally quite satisfactory. Moreover, a principal advantage of the current model is that it is represented by a system of ODEs that allows easy coupling to the neutron kinetic and heat conduction models, as seen in Section 2 where the complete, novel reduced order model for carrying out BWR stability analysis was presented. Equally important is the fact that this ODE system can be handled in a straightforward fashion for carrying out semi-analytical bifurcation analysis using the bifurcation code BIFDD subject of the next section.

#### 4. Results and conditions for in-phase and out-of-phase oscillations

The stability and bifurcation analysis methodology applied in this study is presented in Dokhane (2004). The methodology is based on the present ROM, in form of the developed Fortran code *bwr.f*, in conjunction with the bifurcation code BIFDD (Hassard, 1987).<sup>6</sup> The code *bwr.f* comprises subroutines that numerically evaluate the right

<sup>5</sup> For the Leibstadt NPP, the maximum inlet velocity is 2.67 m/s.

<sup>6</sup> A modified version of the code BIFDD that allows the evaluation of all the 22 eigenvalues and their corresponding eigenvectors at each point on the SB has been used for the present study.

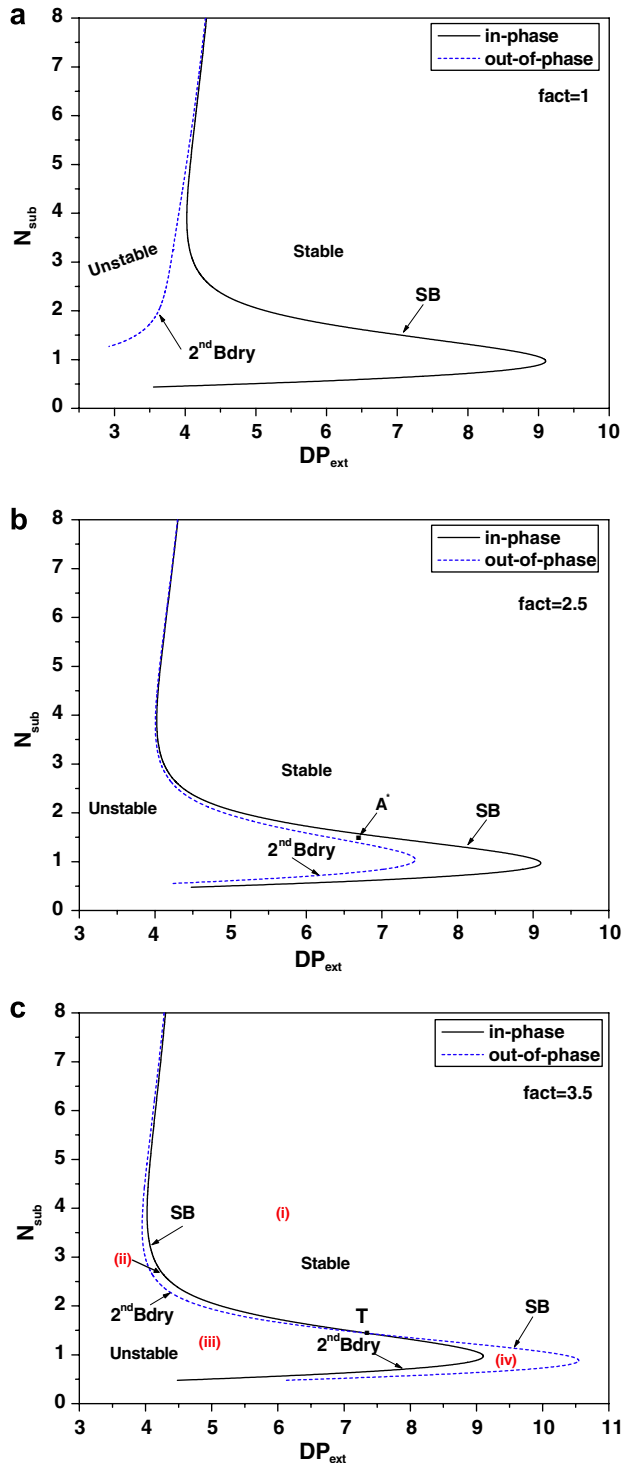


Fig. 3. Stability and a second boundary, and their correspondence to the in-phase and out-of-phase modes for  $\text{fact} = 1, 2.5$  and  $3.5$ . In (a) and (b), the stability boundary corresponds entirely to the in-phase mode and the second boundary corresponds entirely to the out-of-phase mode, while in (c) the stability boundary corresponds to the in-phase mode for  $N_{\text{sub}} > 1.44$  and to the out-of-phase mode for  $N_{\text{sub}} < 1.44$ .

hand side of the set of nonlinear ODEs as well as the Jacobian matrix. The Fortran code *bwr.f* allows any one of the system parameters to be selected as the bifurcation parameter. A second parameter is then incremented in small

steps, and the critical values of the bifurcation parameter and the associated bifurcation characteristics are evaluated. Thus, the entire stability boundary in two-dimensional parameter space can be determined.

The two principal operating parameters chosen for the current stability analysis are  $N_{\text{sub}}$  and  $DP_{\text{ext}}$ , the channel inlet subcooling number, and the external pressure drop across the two channels, respectively, *i.e.* the stability boundaries are presented in the  $N_{\text{sub}} - DP_{\text{ext}}$  parameter space. Note that the same parameter plane was used previously by Karve (1998). This allows a systematic comparison and validation (for the special case of HEM<sup>7</sup>) of the current ROM against the Karve model. In addition, these SBs can be transformed to the more practical power-flow map used by the plant operator.

Currently, we consider a gain of the feedback reactivities for different coupling modes as follows:  $\text{fact}_{11} = \text{fact}_{00} = 1$  and  $\text{fact}_{01} = \text{fact}_{10} = \text{fact}$ , with  $\text{fact} \geq 1$ . This enables an amplification of the feedback reactivities for the coupling between the fundamental and the first modes ( $\rho_{10}, \rho_{01}$ ) by an amount equal to  $\text{fact}$ .<sup>8</sup> One can thus compensate for the current feedback reactivity model's underestimation of the values of the feedback reactivities for the coupling between the fundamental and first modes (Dokhane, 2004).

Besides the semi-analytical bifurcation analysis presented in Section 4.2, direct numerical integration of the set of nonlinear ODEs has been carried out (Section 4.3) to allow an independent confirmation of the results, as well as to determine the system behavior in regions away from the stability boundary where the results of the semi-analytical bifurcation analysis are not applicable, and to determine system behaviour for large times even when operating close to the SB in regions where results of stability analysis may be applicable.

#### 4.1. Mathematical basis for interpretation of results

The present subsection briefly reviews the mathematical basis used to interpret the results obtained. The detailed investigations carried out, *e.g.* to determine as to which oscillation mode is excited during the loss of stability, are described in Section 4.2.

The first boundary corresponds to points in the parameter space at which the real part of the largest pair of complex conjugate eigenvalues is equal to zero, while the second boundary corresponds to points in the parameter space at which the real part of the second largest pair of eigenvalues is equal to zero. In other words, the first boundary is a stability boundary (SB) that corresponds to the occurrence of a PAH bifurcation while the second one is associated with the occurrence of a secondary

<sup>7</sup> Homogenous equilibrium model.

<sup>8</sup> This is a common method, used by many other researchers (Mueño-Cobo et al., 1996; Zhou and Rizwan-uddin, 2002), in order to simulate the excitation of the out-of-phase oscillation mode at some specific OPs, when ROMs are used.

PAH bifurcation, or a so-called Neimark bifurcation. The second boundary has little relevance to the stability of the system, since the system is already unstable once the first boundary (SB) has been crossed. However, it is crucial for understanding the switch between the in-phase and out-of-phase oscillation modes.

In the following, we show the necessity of making a distinction between the fundamental and first azimuthal neutronics modes, on the one hand, and in-phase and out-of-phase mode instabilities on the other hand. Thus, it will be seen that an in-phase instability implies growing neutron oscillations that are *dominated* by the fundamental neutronics mode. The first azimuthal neutronics mode may also be unstable and growing, but its contribution to the total neutron population is relatively insignificant. Similarly, an out-of-phase instability implies growing neutronics oscillations that are *dominated* by the first azimuthal mode. In this case, the fundamental neutronics mode may also be unstable and growing, but its contribution to the total neutron population is relatively insignificant. The question to be answered is as to whether the complex conjugate pair of eigenvalues that first crosses the imaginary axis corresponds to an in-phase or to an out-of-phase mode instability, or, in other words, as to whether it is possible to associate a particular pair of eigenvalues with a particular kind of (in-phase or out-of-phase) instability.

Zhou and Rizwan-uddin (2002) reported that complex conjugate eigenvalues with the largest and second largest real parts are responsible for the in-phase and out-of-phase mode oscillations. They examined the magnitude of the elements corresponding to the fundamental and first modes in the eigenvectors in order to identify the associated mode of oscillation. In the current analysis, it has been found that, in addition to the elements corresponding to the fundamental and first modes, eigenvector elements corresponding to the thermal-hydraulic and heat conduction variables also have distinct properties for the two eigenvectors associated to the two relevant complex conjugate eigenvalues, *i.e.* those with the largest and second largest real parts. In this context, the two eigenvectors, called here  $\vec{V}_{in}$  and  $\vec{V}_{out}$ <sup>9</sup> have certain characteristics. Specifically, for  $\vec{V}_{in}$ , these are:

- in-1.* The element corresponding to the fundamental neutronics mode,  $V_{in,n_0}$ , is much larger than the element corresponding to the first mode,  $V_{in,n_1}$ . Moreover, the element corresponding to the fundamental mode in eigenvector  $\vec{V}_{in}$ ,  $V_{in,n_0}$ , is much larger than the corresponding element in eigenvector  $\vec{V}_{out}$ ,  $V_{out,n_0}$ . This was also reported by Zhou and Rizwan-uddin (2002).
- in-2.* The elements corresponding to the thermal-hydraulic/heat conduction variables in the first channel have the same sign and the same absolute value as the corresponding elements of the second channel.

In the case of the other eigenvector,  $\vec{V}_{out}$ , the characteristic properties are:

- out-1.* The element corresponding to the first neutronics mode,  $V_{out,n_1}$ , is much larger than the element corresponding to the fundamental mode,  $V_{out,n_0}$ . Moreover, the element corresponding to the first mode in eigenvector  $\vec{V}_{in}$ ,  $V_{in,n_1}$ , is much smaller than the corresponding element in eigenvector  $\vec{V}_{out}$ ,  $V_{out,n_1}$ . This was also reported by Zhou and Rizwan-uddin (2002).
- out-2.* The elements corresponding to the thermal-hydraulic/heat conduction variables in the first channel are of opposite sign and have the same absolute value as the corresponding elements of the second channel.

Moreover, the elements corresponding to the thermal-hydraulic and heat conduction variables in eigenvector  $\vec{V}_{in}$  have values of the same order of magnitude as those of the corresponding elements in eigenvector  $\vec{V}_{out}$ .

An analysis of the impact of the eigenvector elements for both eigenvectors ( $\vec{V}_{in}$  and  $\vec{V}_{out}$ ) on the behaviour of the system, *i.e.* the evolution of the system variables with time, close to the steady-state solutions is presented below.

Suppose the linearized system of the set of nonlinear ODEs (13) is

$$\frac{d\vec{X}(t)}{dt} = A \cdot \vec{X}(t) \quad (15)$$

where  $A$  is the Jacobian matrix and  $\vec{X}(t)$  is the vector variable. To solve this system of equations, suppose the matrix  $A$  can be diagonalized. For this, the eigenvalues  $\lambda_i = \sigma_i \pm i\omega_i$  and their corresponding eigenvectors  $\vec{V}_i$  are evaluated. Then the solution of the linearized system can be written as:

$$\vec{X}(t) = \vec{X} + \sum_{i=1}^{22} c_i \vec{V}_i e^{\lambda_i t} \quad (16)$$

where  $\vec{X}$  is the steady-state variable vector and  $c_i$  is a constant that can be evaluated from the initial condition problem.

Generally speaking, it is well known that the dynamical system is asymptotically stable, *i.e.* the oscillation amplitudes of all the variables asymptotically decay with time, only if real parts of all the eigenvalues of the Jacobian are negative. On the other hand, the system is asymptotically unstable, *i.e.* the oscillation amplitudes of some variables asymptotically grow with time, if the real part of at least one eigenvalue is positive.

Suppose that the two complex conjugate eigenvalues of the Jacobian matrix with the largest real parts corresponding to the eigenvectors  $\vec{V}_{in}$  and  $\vec{V}_{out}$  are denoted by  $\lambda_{in}$  and  $\lambda_{out}$ . With  $\lambda_{in} = \sigma_{in} \pm i\omega_{in}$  and  $\lambda_{out} = \sigma_{out} \pm i\omega_{out}$ . The asymptotic solution can then be approximated by:

<sup>9</sup> These eigenvectors can be associated either to the complex conjugate pair of eigenvalues with largest real part or to that with the second largest real part.

$$\vec{X}(t) \cong \vec{X} + c_{\text{out}} \vec{V}_{\text{out}} e^{\lambda_{\text{out}} t} + c_{\text{in}} \vec{V}_{\text{in}} e^{\lambda_{\text{in}} t} \quad (17)$$

Hence, the solution for the fundamental and the first modes can be expressed as

$$n_0(t) \cong \tilde{n}_0 + c_{\text{out}} V_{\text{out},n_0} e^{\lambda_{\text{out}} t} + c_{\text{in}} V_{\text{in},n_0} e^{\lambda_{\text{in}} t} \quad (18)$$

$$n_1(t) \cong \tilde{n}_1 + c_{\text{out}} V_{\text{out},n_1} e^{\lambda_{\text{out}} t} + c_{\text{in}} V_{\text{in},n_1} e^{\lambda_{\text{in}} t} \quad (19)$$

For  $c_{\text{in}}$  and  $c_{\text{out}}$  approximately equal, the relative magnitude of the fundamental and first azimuthal modes will depend upon the magnitude of the eigenvector elements  $V_{\text{out},n_0}$ ,  $V_{\text{in},n_0}$ ,  $V_{\text{out},n_1}$ , and  $V_{\text{in},n_1}$  corresponding to the phase variables  $n_0(t)$  and  $n_1(t)$ .

Similar to the evolution of the fundamental and first azimuthal neutronics modes, the time evolution of the liquid inlet velocities in channels 1 and 2, as example of the thermal-hydraulic variables, can also be written as:

$$v_{\text{inlet},1}(t) \cong \tilde{v}_{\text{inlet},1} + c_{\text{out}} V_{\text{out},v_{\text{inlet},1}} e^{\lambda_{\text{out}} t} + c_{\text{in}} V_{\text{in},v_{\text{inlet},1}} e^{\lambda_{\text{in}} t} \quad (20)$$

$$v_{\text{inlet},2}(t) \cong \tilde{v}_{\text{inlet},2} + c_{\text{out}} V_{\text{out},v_{\text{inlet},2}} e^{\lambda_{\text{out}} t} + c_{\text{in}} V_{\text{in},v_{\text{inlet},2}} e^{\lambda_{\text{in}} t} \quad (21)$$

where  $(V_{\text{out},v_{\text{inlet},1}}, V_{\text{in},v_{\text{inlet},1}})$  and  $(V_{\text{out},v_{\text{inlet},2}}, V_{\text{in},v_{\text{inlet},2}})$  are respectively the eigenvector elements of the two eigenvectors corresponding to the phase variables  $v_{\text{inlet},1}(t)$  and  $v_{\text{inlet},2}(t)$ . It should be noted that  $\tilde{v}_{\text{inlet},1} = \tilde{v}_{\text{inlet},2}$  because the two channels are identical from the thermal-hydraulic point of view.

In the above context, two different cases of BWR instability can be distinguished. These are:

**CASE I:**  $\sigma_{\text{in}} > 0$  and  $\sigma_i < 0$  for  $\forall i = 1, 2, \dots, n$  and  $i \neq \text{in}$

In this case, the state (behaviour) of the system is dictated by the eigenvector  $\vec{V}_{\text{in}}$ . In specific terms, Eqs. (18) and (19) show that, since  $V_{\text{in},n_0} \gg V_{\text{in},n_1}$  (property *in-1*), the oscillation amplitude of the fundamental mode  $n_0(t)$  is much larger than that of the first azimuthal mode  $n_1(t)$ . Furthermore, as stated earlier, the elements of the eigenvector  $\vec{V}_{\text{in}}$  corresponding to the inlet velocity variables in channel 1 ( $V_{\text{in},v_{\text{inlet},1}}$ ) and channel 2 ( $V_{\text{in},v_{\text{inlet},2}}$ ) are found to have the same sign and the same absolute value (property *in-2*). Therefore, referring to Eqs. (20) and (21), the inlet velocities in the two channels oscillate in an in-phase manner. This clearly shows that the oscillation mode, associated with the eigenvector  $\vec{V}_{\text{in}}$ , is in-phase.

It needs to be stressed that, even if out-of-phase oscillations are not excited in this case, the oscillation amplitude of the first mode grows with time asymptotically. It may actually decay initially<sup>10</sup>, but then should grow asymptotically. A possible initial decay of the oscillation amplitude of the first neutronics mode can be explained by the contribution of the term associated with the second pair of complex eigenvalues that has a negative real part. In other words, since  $\sigma_{\text{in}} > 0$  and  $\sigma_{\text{out}} < 0$ , the  $\lambda_{\text{out}}$  term in Eq. (19),  $c_{\text{out}} V_{\text{out},n_1} e^{\lambda_{\text{out}} t}$ , may be dominant in the initial transient time interval, because, as reported earlier,  $V_{\text{out},n_1}$  is found to be much larger than  $V_{\text{in},n_1}$  (about 100 times) and, conse-

quently, decaying oscillations of the first neutronics mode are observed. The time evolution of the thermal-hydraulic and heat conduction variables, however, is always growing because here the  $\lambda_{\text{out}}$  term of the second pair of complex eigenvalues corresponding to these variables (e.g. in Eqs. (20) and (21)) is almost negligible even in the initial time interval.

**CASE II:**  $\sigma_{\text{out}} > 0$  and  $\sigma_i < 0$  for  $\forall i = 1, 2, \dots, n$  and  $i \neq \text{out}$

In this case, the state of the system is dictated by the eigenvector  $\vec{V}_{\text{out}}$ . In specific terms, Eqs. (18) and (19) show that, since  $V_{\text{out},n_1} \gg V_{\text{out},n_0}$  (property *out-1*), the oscillation amplitude of the first azimuthal mode  $n_1(t)$  is much larger than that of the fundamental mode  $n_0(t)$ . Furthermore, as stated earlier, the elements of the eigenvector  $\vec{V}_{\text{out}}$  corresponding to the inlet velocity variables in channel 1 ( $V_{\text{out},v_{\text{inlet},1}}$ ) and channel 2 ( $V_{\text{out},v_{\text{inlet},2}}$ ) are found to have opposite signs and the same absolute value (property *out-2*). Therefore, referring to Eqs. (20) and (21), the inlet velocities in the two channels oscillate in an out-of-phase manner. This clearly shows that the oscillation mode, associated with the eigenvector  $\vec{V}_{\text{out}}$ , is out-of-phase.

Again it needs to be emphasized that, even if in-phase oscillations are not excited in this case, the oscillation amplitude of the fundamental neutronics mode grows with time asymptotically, i.e. it may decay initially but then should grow asymptotically. A possible initial decay of the oscillation amplitude of the fundamental neutronics mode can be explained by the contribution of the term associated with the second pair of complex eigenvalues that has a negative real part. In other words, since  $\sigma_{\text{out}} > 0$  and  $\sigma_{\text{in}} < 0$ , the  $\lambda_{\text{in}}$  term in Eq. (18),  $c_{\text{in}} V_{\text{in},n_0} e^{\lambda_{\text{in}} t}$ , may be dominant in the initial transient time interval, because, as reported earlier,  $V_{\text{in},n_0}$  is found to be much larger than  $V_{\text{out},n_0}$  (more than 100 times) and, consequently, decaying oscillations of the fundamental neutronics mode are observed. However, this is not the case for the time evolution of the other thermal-hydraulic and heat conduction variables, i.e. there are no decaying oscillations in the initial time interval because here the  $\lambda_{\text{in}}$  term of the second pair of complex eigenvalues corresponding to these variables (e.g. in Eqs. (20) and (21)) is almost negligible even initially.

The analysis carried out above clearly demonstrates that the eigenvector  $\vec{V}_{\text{in}}$  (properties *in-1* and *in-2*) is associated with the in-phase mode and that the eigenvector  $\vec{V}_{\text{out}}$  (properties *out-1* and *out-2*) is associated with the out-of-phase mode. This, in effect, corresponds to the fact that in-phase and out-of-phase oscillation modes are whole-system mechanisms.

#### 4.2. Semi-analytical bifurcation analysis

The stability and bifurcation analyses reported in this subsection have been carried out using the current 22-equation ROM with the drift flux parameters set to correspond to a HEM, i.e.  $C_0 = 1$  and  $V_{g_j} = 0.0$ . This has been done mainly for a more clear understanding of the different

<sup>10</sup> It may happen that the asymptotic time is very large, which could make the “initial” interval very long.

phenomena observed. The conclusions drawn regarding the mechanisms for in-phase and out-of-phase oscillations are, however, independent of the degree of modelling detail, *viz.* DFM or HEM. Employing the typical BWR numerical values for design and operating parameters (Dokhane, 2004) mentioned earlier, the first (stability) and the second boundaries are presented for different values of the reactivity feedback for the coupling between the fundamental and first modes, *i.e.* for different values of the bifurcation parameter fact.

Shown in Fig. 3 are the first and the second boundaries in the  $N_{\text{sub}} - DP_{\text{ext}}$  plane for the bifurcation parameter fact equal to 1, 2.5 and 3.5. Fig. 3a shows that, for fact = 1, the entire stability boundary is associated with the in-phase mode, while the entire second boundary is associated with the out-of-phase mode. The two boundaries are very close for  $N_{\text{sub}} > 4$ , but separate considerably from each other for lower values of  $N_{\text{sub}}$ . Comparing Fig. 3a and b, it is seen that increasing the value of fact to 2.5 shifts the second boundary (corresponding to the out-of-phase mode) closer and closer to the stability boundary (corresponding to the in-phase mode) even for low values of  $N_{\text{sub}}$ . Fig. 3c shows the case of even higher feedback reactivity for the coupling between the fundamental and first modes (fact = 3.5), in which the two boundaries intersect at point  $T$  ( $DP_{\text{ext}}, N_{\text{sub}} = T(7.38, 1.44)$ ). In this case, the SB corresponds to the in-phase oscillation mode for  $N_{\text{sub}} > 1.44$ , and to the out-of-phase mode for  $N_{\text{sub}} < 1.44$ . In other words, if the system loses its stability by crossing the SB in the region where  $N_{\text{sub}} < 1.44$  (but not crossing the second boundary), the type of instability that will be excited is the out-of-phase oscillation mode. On the other hand, for  $N_{\text{sub}} > 1.44$ , the type of instability that will be encountered is the in-phase oscillation mode. Note that, as illustrated in Fig. 3c, four regions could be distinguished in parameter space: region (i) where both modes are stable; region (ii) where only in-phase is unstable; region (iii) where both modes are unstable; and region (iv) where the in-phase mode is stable while the out-of-phase mode is unstable (see Fig. 3c). These results are similar to those obtained using a simple model by March-Leuba and Blakeman (1991).

Fig. 4 shows the stability boundary and the type of Hopf bifurcation corresponding to different gains of the feedback reactivity for the coupling between the fundamental and first modes. The stability boundaries and the bifurcation curve for fact equalling 1 and 2.5 cannot be distinguished. As seen earlier, further increasing the feedback for the coupling between the fundamental and first modes (fact = 3.5) causes the out-of-phase mode to be excited. Consequently, the branch of the SB for lower values of  $N_{\text{sub}}$  that was associated with the in-phase mode for lower values of fact becomes associated with the out-of-phase mode. The SBs shown in Fig. 4b are the transformed SBs from  $N_{\text{sub}} - DP_{\text{ext}}$  to the steady-state values of neutron number density vs. total inlet velocity (power-flow) plane  $n_{0s} - v_{\text{inlet},s}$ . It is clear, from Fig. 4a and b, that underestimating the feed-

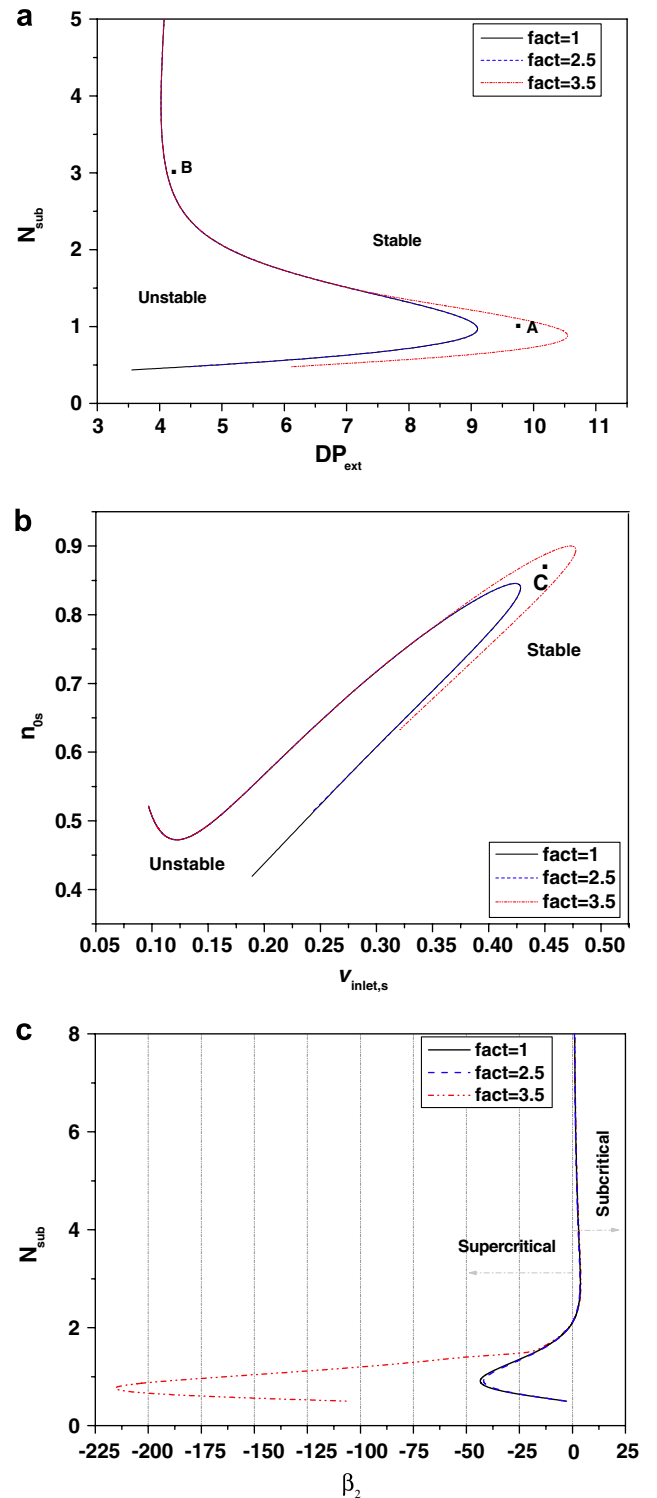


Fig. 4. (a) The stability boundaries for different values of feedback reactivities fact in the  $N_{\text{sub}} - DP_{\text{ext}}$  plane. (b) Transformed stability boundaries in the power-flow map ( $n_{0s}$  and  $v_{\text{inlet},s}$  are the steady-state values of the neutron number density of the fundamental mode and the total inlet velocity, respectively). (c) Nature of PAH bifurcation in the  $N_{\text{sub}} - \beta_2$  plane. Bifurcation is supercritical for  $\beta_2 < 0$ , and subcritical for  $\beta_2 > 0$ .

back reactivity for the coupling between the fundamental and first modes leads to non-conservative results. For instance, point C, which is predicted to be a completely

stable operational point under  $\text{fact} = 1$  conditions, becomes an out-of-phase unstable operating point if the gain of the feedback reactivity coupling between the fundamental and first modes is increased sufficiently to represent realistic conditions corresponding, for instance, to a bowl-shaped radial power distribution (Miró et al., 2000).<sup>11</sup> In Fig. 4c,  $\beta_2$  is the parameter that determines the stability of the periodic oscillations. If  $\beta_2 < 0$ , the periodic solution is stable, *i.e.* supercritical bifurcation, while if  $\beta_2 > 0$  the periodic solution is unstable, *i.e.* subcritical bifurcation. For  $\text{fact} = 1, 2$  and  $3.5$ , subcritical bifurcation is expected for  $N_{\text{sub}} > 2.1$ , and supercritical for  $N_{\text{sub}} < 2.1$ . The sudden jump in  $\beta_2$  for  $\text{fact} = 3.5$  is due to the intersection of the corresponding in-phase and out-of-phase boundaries, reported earlier (see Fig. 3c). In other words, for  $N_{\text{sub}} > 1.44$ , the bifurcation branch corresponds to the pair of complex eigenvalues associated with the in-phase mode that crosses first the imaginary axis, while for  $N_{\text{sub}} < 1.44$ , it corresponds to the pair of complex eigenvalues associated with the out-of-phase mode that crosses first the imaginary axis. Results of the bifurcation analysis are consistent with those reported by Zhou and Rizwan-uddin (2002).

Points *A* and *B* shown in Fig. 4a are two operational points that will be investigated, in Section 4.3, using numerical integration of the set of system equations, point *A* is stable for  $\text{fact}$  equal to 1 or 2.5. However, it is out-of-phase unstable<sup>12</sup> for  $\text{fact} = 3.5$ . In addition, point *A* is in the region where a supercritical PAH bifurcation is expected (see Fig. 4c). Therefore, an out-of-phase stable limit cycle oscillation is expected here. Point *B*, for all the considered values of  $\text{fact}$ , is located in a stable region where subcritical bifurcation is expected.

It should be pointed out that typical values of the subcooling number  $N_{\text{sub}}$ , for normal operational conditions for a BWR, cannot exceed 2.0, which corresponds to 30 °C temperature difference between the inlet liquid temperature and the saturation temperature. In the current study, higher values of  $N_{\text{sub}}$  were also investigated in order to try to understand the physical mechanisms behind the transition between the in-phase and out-of-phase modes as a given parameter is changed, especially in a region where the two boundaries are very close to each other.

#### 4.3. Numerical simulation

For independent confirmation of the results of the bifurcation analyses, and to evaluate the system behaviour in regions away from the SB, a Matlab code has been developed to numerically integrate the set of the 22 ODEs using the Gear's algorithm. Results are presented here for parameter values corresponding to the operational points *A* and *B* shown in Fig. 4a with  $\text{fact} = 3.5$  and point *A\** shown in Fig. 3b (with  $\text{fact} = 2.5$ ). Fig. 5 shows the time

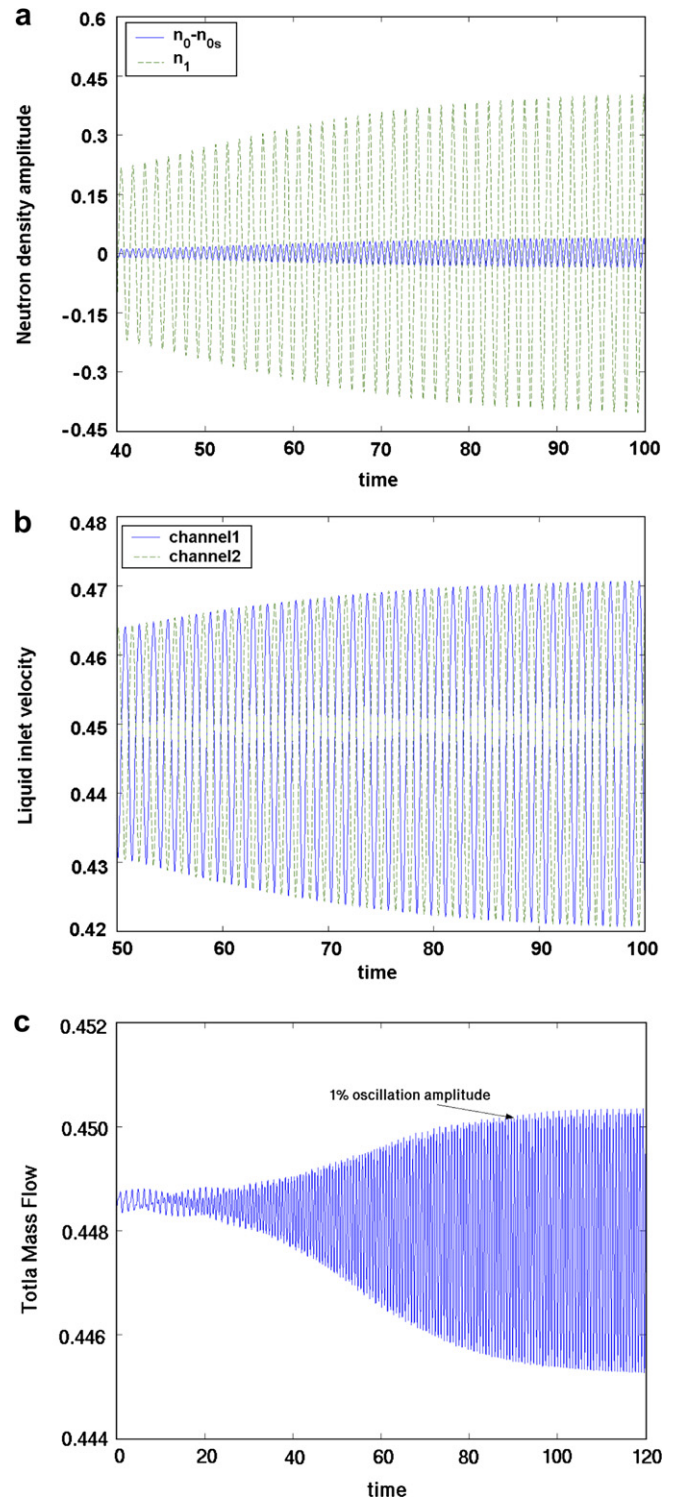


Fig. 5. (a) Time evolution of  $(n_0(t) - n_{0s})$  and  $n_1(t)$  at point *A* (Fig. 4). (b) Time evolution of inlet flow velocity in the two channels. (c) Time evolution of the total inlet mass flow rate.

evolution of normalized components of the fundamental ( $n_0(t)$ ) and the first modes ( $n_1(t)$ ), the inlet liquid velocity in both channels ( $v_{\text{inlet},1}$  and  $v_{\text{inlet},2}$ ), and the total liquid inlet velocity  $v_{\text{inlet}}$ , with parameter values corresponding to point *A*. As expected, at point *A*, the system is out-of-phase unstable but in-phase stable, *i.e.* the out-of-phase

<sup>11</sup> Resulting, for example, from a certain control rod configuration.

<sup>12</sup> This means that the out-of-phase mode is excited at the operational point *A*.

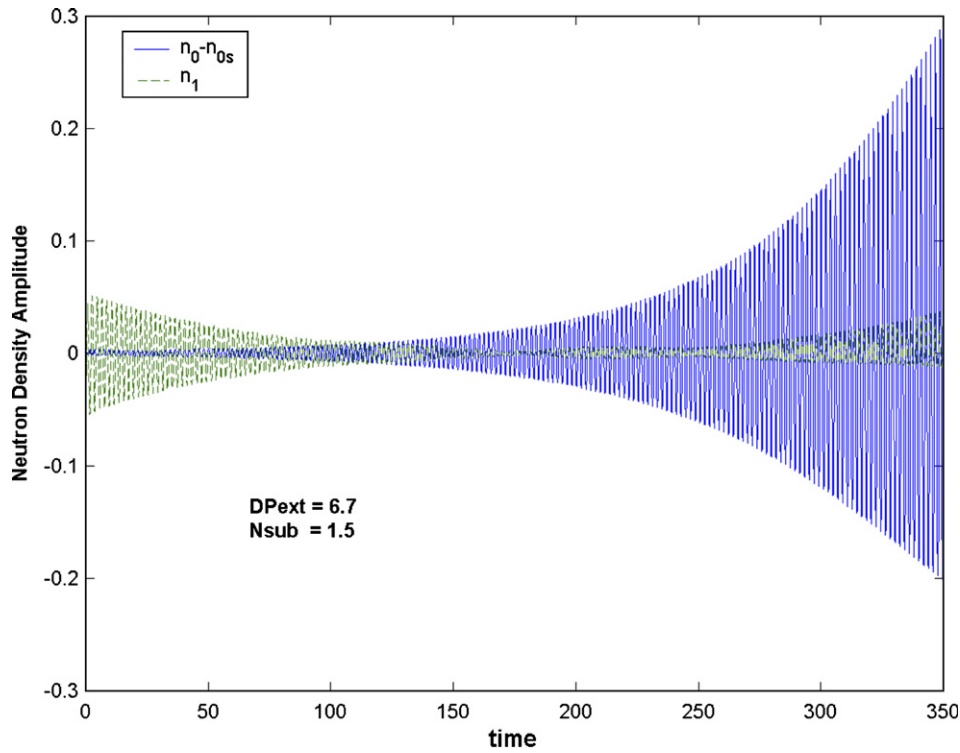


Fig. 6. Time evolution of  $n_0(t) - n_{0s}$  and  $n_1(t)$  at point  $A^*$  in Fig. 3(b). The amplitude of the first mode is decaying from 0 to 170 s, then starts to grow but with much smaller amplitude than that of the fundamental mode.

mode is dominant. The oscillation amplitude of the first mode is larger than that of the fundamental mode (Fig. 5a). Moreover, point  $A$  is in the supercritical PAH bifurcation region. Hence, the oscillation amplitude for each of the variables grows to a stable limit cycle.

Fig. 5b clearly shows the out-of-phase mode oscillation between the inlet liquid velocities of the two channels. The total mass flow ( $v_{inlet}$ ) is oscillating with very small amplitude (1%) and can, as such, be considered constant (Fig. 5c). This agrees with previous findings that in an out-of-phase oscillation mode the total mass flow remains almost constant, although the individual channel mass flows are oscillating (March-Leuba and Blakeman, 1991). This is because the two oscillating core regions adjust their flows to maintain the pressure drop across the core constant in time and in space. In fact, the 1% oscillation amplitude of the total flow rate is related to the fundamental mode that shows very small stable limit cycle oscillation amplitude. It should be pointed out that, although the in-phase mode is not excited<sup>13</sup> at point  $A$ , the oscillation amplitude of the fundamental mode is increasing but with very small amplitude compared to the first mode.

Fig. 6 shows the results of numerical integration for the operational point  $A^*$  in Fig. 3b. It is clearly seen that, although the out-of-phase mode is not excited<sup>14</sup> (only the

in-phase is), the first mode amplitude grows asymptotically (time  $> 170$  s) but with an amplitude much smaller than that of the fundamental mode. This can be explained by the arguments presented earlier, *viz.* that in the initial time interval  $[0, 170$  s] the first azimuthal neutronics mode amplitude is decaying because of the dominance of the term associated with the second pair of complex eigenvalues that have negative real parts (associated in this case with the out-of-phase mode,  $c_{out} V_{out, n_1} e^{\lambda_{out} t}$ ), and that later the first mode amplitude grows with time because of the dominance of the term associated with the first pair of complex eigenvalues that have positive real parts (associated in this case with the in-phase mode,  $c_{in} V_{in, n_1} e^{\lambda_{in} t}$ ).

The above discussion for points  $A$  and  $A^*$  clearly shows the distinction between in-phase and out-of-phase modes, on one hand, and the fundamental and the first azimuthal neutronics modes on the other. Recall that according to our definition of in-phase and out-of-phase modes of oscillations, they are intrinsic states of the “system” and are decoupled from the stability of fundamental and first azimuthal neutronics modes. Whether the in-phase and/or out-of-phase modes are “stable” or “unstable” depends on the real part of their corresponding pair of complex conjugate eigenvalues. Hence, it is possible that while the fundamental (first) neutronics mode is unstable, the in-phase (out-of-phase) mode is stable. An unstable fundamental neutronics mode and a “stable” in-phase mode simply means that it is the out-of-phase mode that is unstable leading to oscillations that are primarily out-of-phase.

<sup>13</sup> This means that the real part of the pair of complex eigenvalues associated with the in-phase mode is negative.

<sup>14</sup> This means that the real part of the pair of complex eigenvalues associated with the out-of-phase mode is negative.

As regards point *B* in Fig. 4a, it is clear that here the SB corresponds to the in-phase mode, the second boundary being associated with the out-of-phase mode (see Fig. 3c), and that the two are very close. Point *B* is in the stable region and close to the SB, and the type of

PAH bifurcation to be expected is subcritical (Fig. 4c). Therefore, beside the stable fixed point, an unstable limit cycle is predicted. Numerical simulations confirm these findings, as shown in Figs. 7 and 8. The small amplitude perturbation in Fig. 7 ( $\delta v_{\text{inlet},1} = 0.05$ ) decays to the fixed

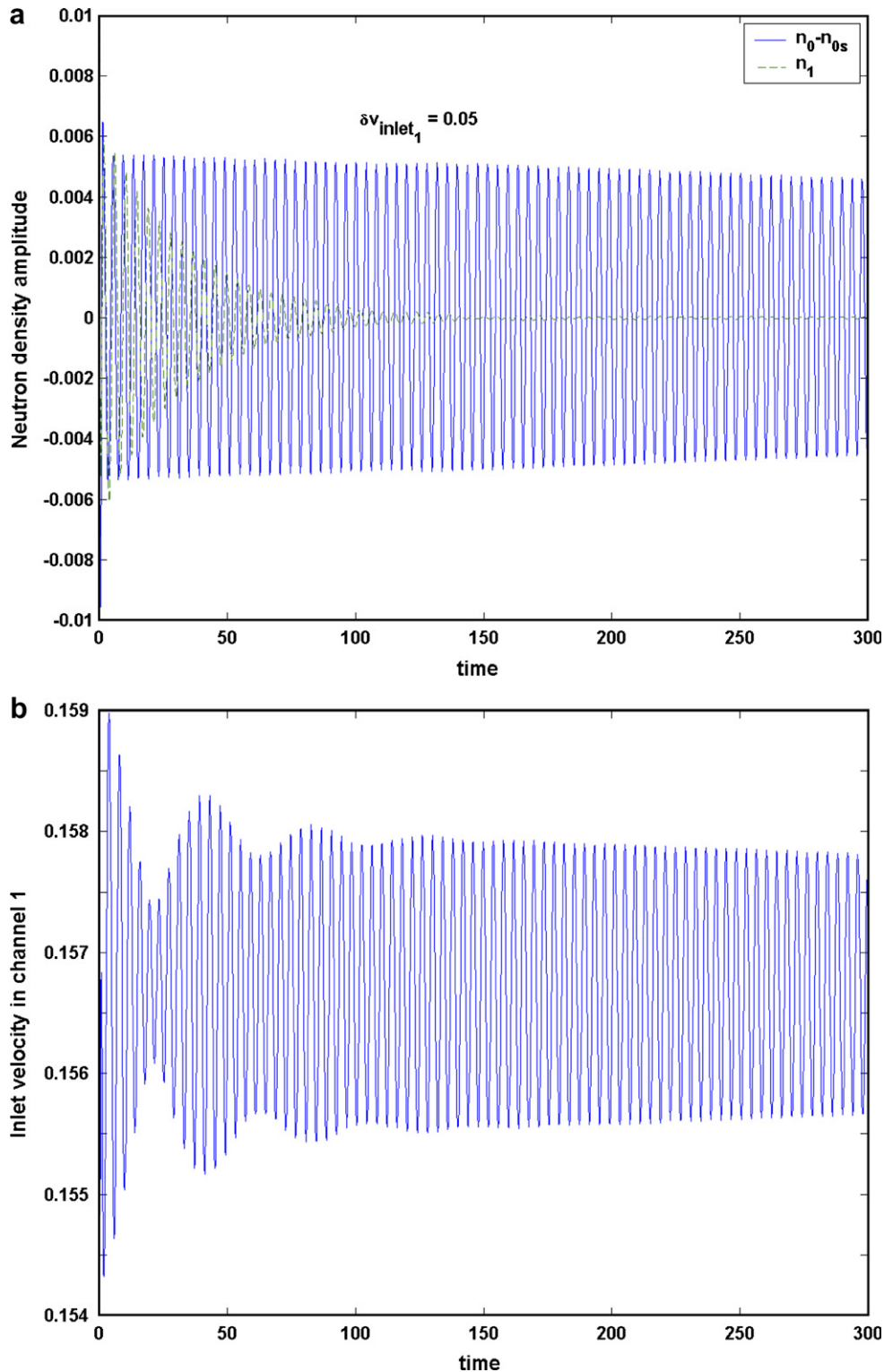


Fig. 7. (a) Time evolution of  $n_0(t) - n_{0s}$  and  $n_1(t)$  at point *B* for small amplitude perturbation. (b) Corresponding time evolution of inlet flow velocity in channel 1.

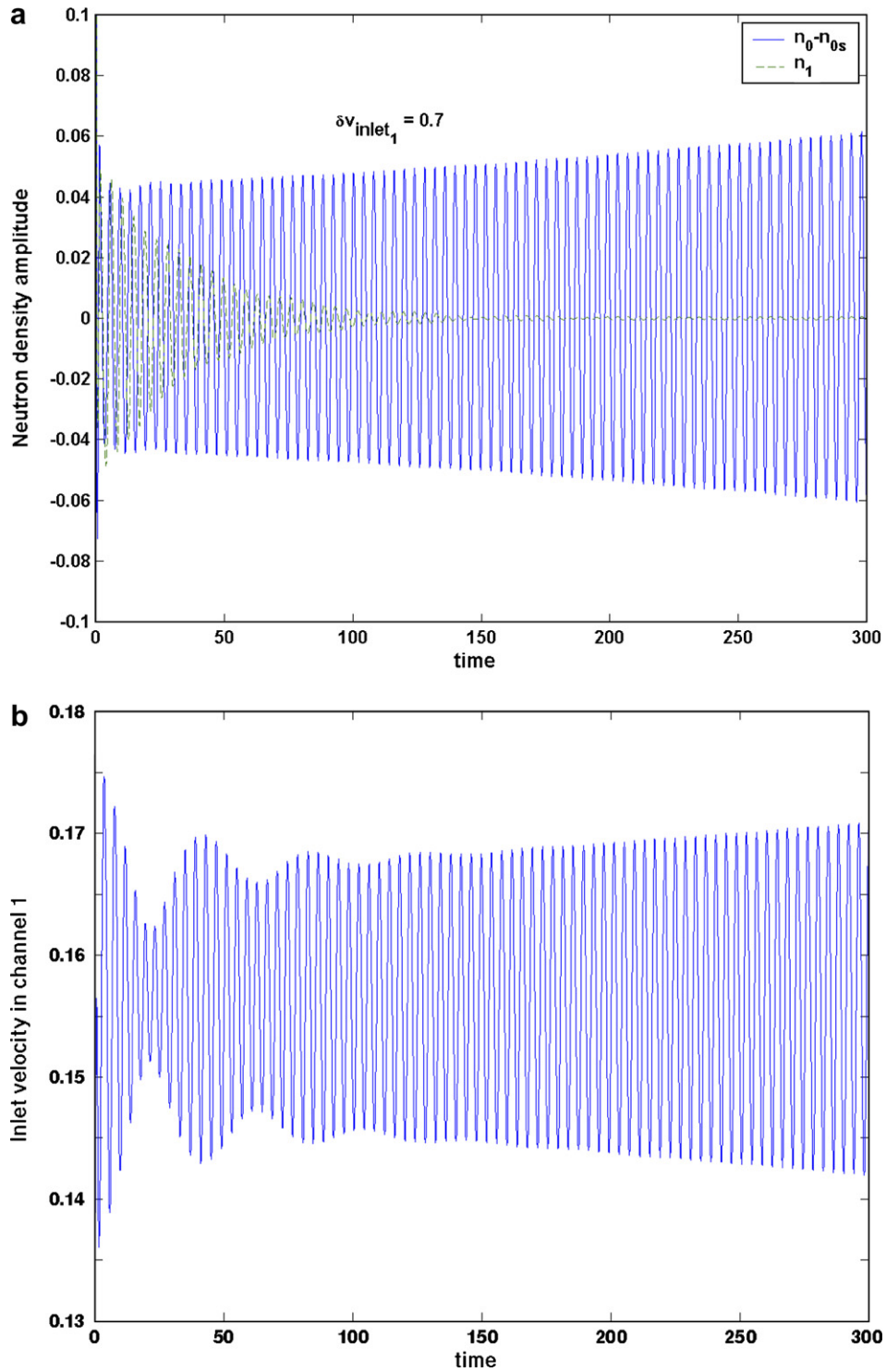


Fig. 8. (a) Time evolution of  $n_0(t) - n_{0s}$  and  $n_1(t)$  at point  $B$  for large amplitude perturbation. (b) Corresponding time evolution of inlet flow velocity in channel 1.

point, and the large amplitude perturbation ( $\delta v_{inlet,1} = 0.7$ ) in Fig. 8 leads to growing amplitude oscillations for  $n_0(t)$  and  $v_{inlet,1}(t)$ . However, in both cases, the first mode decreases rapidly. As discussed above, this is because of the dominance of the term associated with the second pair of complex conjugate eigenvalues,  $c_{out} V_{out,m1} e^{\lambda_{out}^2 t}$ , with  $\text{Re}(\lambda_{out}) < 0$ .

The evolution of flow inlet velocity in channel 1 is seen to experience the beating phenomenon<sup>15</sup> in the first 150 s (Figs. 7b and 8b), because during this time interval, the term

<sup>15</sup> It is well known that the beating phenomenon is observed when two frequencies or more, with very close values, exist.

associated with the pair of complex conjugate eigenvalues associated with the out-of-phase mode ( $c_{\text{out}} V_{\text{out},v_{\text{inlet},1}} e^{\lambda_{\text{out}} t}$ ) has a magnitude comparable to that associated with the in-phase mode term ( $c_{\text{in}} V_{\text{in},v_{\text{inlet},1}} e^{\lambda_{\text{in}} t}$ ).

## 5. Summary and conclusions

An extended reduced order model has been developed to simulate the different types of instabilities encountered in BWRs, *viz.* nuclear-coupled thermal-hydraulic instabilities in the reactor core. The 22-ODE model comprises three main parts: spatial lambda-mode neutron kinetics with the fundamental and first azimuthal modes, fuel heat conduction dynamics, and core thermal-hydraulics based on a drift flux model representation of the two-phase flow.

The thermal-hydraulic part of the model has been validated against appropriate experimental data and also compared with several other analytical models, developed earlier for simulating thermal-hydraulic instabilities. This validation study shows that thermal-hydraulic model predictions are in good agreement with the experimental results for large values of  $N_{\text{sub}}$  and, for lower values, agree better than most of the earlier analytical models. In particular, it was seen that the present extension of the Karve ROM, employing a drift flux model for two-phase flow (instead of a homogeneous equilibrium model), provided considerably improved results, especially for high inlet mass flow rates.

Stability and semi-analytical bifurcation analyses have been performed using the bifurcation analysis code BIFDD to determine the stability limits for both in-phase and out-of-phase oscillation modes, as well as the nature of PAH bifurcation. The results obtained show that both sub- and supercritical PAH bifurcations are encountered in different regions of the parameter space. Furthermore, it has been seen also that analysing the properties of the elements of the eigenvectors gives complete information on the type of oscillation mode (in-phase or out-of-phase) without solving the set of ODEs. A clear distinction is thereby made between in-phase and out-of-phase oscillation modes, on the one hand, and the fundamental and first azimuthal neutronics modes on the other hand.

Numerical integration of the set of 22 ODEs has been carried out using a Matlab code based on the Gear's algorithm to solve stiff problems. The results obtained confirmed the findings of the semi-analytical bifurcation analysis.

## Acknowledgements

This research has been conducted in the framework of the nuclear safety analysis project STARS at PSI and, as such, has been partly sponsored by the Swiss Federal Nuclear Safety Inspectorate (HSK). Rizwan-uddin would like to acknowledge support from the US Department of Energy under a Nuclear Engineering Education Research grant.

## References

- Dokhane, A., 2004. BWR stability and bifurcation analysis using a novel reduced order model and the system code RAMONA. Doctoral Thesis No. 2927, EPFL, Switzerland. <http://library.epfl.ch/theses/?nr=2927>.
- Dokhane, A., Hennig, D., Rizwan-uddin, Chawla, R., 2005. Semi-analytical bifurcation analysis of two-phase flow in a heated channel. *Int. J. Bifurc. Chaos* 15 (8), 2395–2409.
- Dokhane, A., Hennig, D., Rizwan-uddin, Chawla, R., 2007. BWR stability and bifurcation analysis using reduced order models and system codes: identification of a subcritical Hopf bifurcation using RAMONA. *Ann. Nucl. Energy*, submitted for publication.
- Dykhuizen, R.C., Roy, R.P., Kalra, S.P., 1986. A linear time-domain two-fluid model analysis of dynamic instability in boiling flow systems. *J. Heat Transfer* 108, 222.
- Hassard, B.D., 1987. A code for Hopf bifurcation analysis of autonomous delay-differential equations. *Proc. Oscillations, Bifurcation and Chaos*. Canadian Mathematical Society, p. 447.
- Hassard, B.D., Kazarinoff, N.D., Wan, Y.H., 1981. *Theory and Application of Hopf Bifurcation*. Cambridge University Press, New York.
- Hennig, D., 1999. A study of boiling water reactor stability behaviour. *Nucl. Technol.* 125, 10.
- Ishii, M., Zuber, N., 1970. Thermally induced flow instabilities in two-phase mixtures. In: *Heat Transfer*, vol. V. Elsevier Publishing Co., p. B11.
- Karve, A.A., 1998. Nuclear-coupled thermal-hydraulic stability analysis of boiling water reactors. Ph.D. dissertation, Virginia University.
- Karve, A.A., Rizwan-uddin, Dorning, J.J., 1997. Out-of-phase oscillations in boiling water reactors. In: *Proc. of the Joint Int. Conf. on Mathematical Methods and Super-Computing*, Saratoga, Springs, NY, October 5–9, vol. 2, p. 1633.
- March-Leuba, J., Blakeman, E.D., 1991. A mechanism for out-of-phase power instabilities in boiling water reactors. *Nucl. Eng. Des.* 107, 173.
- March-Leuba, J., Cacuci, D.G., Perez, R.B., 1986a. Nonlinear dynamics and stability of boiling water reactors: Part 1 – Qualitative analysis. *Nucl. Sci. Eng.* 93, 111.
- March-Leuba, J., Cacuci, D.G., Perez, R.B., 1986b. Nonlinear dynamics and stability of boiling water reactors: Part 2 – Quantitative analysis. *Nucl. Sci. Eng.* 93, 124.
- Miró, R., Ginestar, G., Hennig, D., Verdú, G., 2000. On the regional oscillation phenomena in BWRs. *Prog. Nucl. Energy* 36 (2), 189.
- Muñoz-Cobo, J.L., Verdú, G., 1991. Application of Hopf bifurcation theory and variational methods to the study of limit cycles in boiling water reactors. *Ann. Nucl. Energy* 18 (5), 269.
- Muñoz-Cobo, J.L., Pérez, R.B., Ginestar, D., Escrivá, A., Verdú, G., 1996. Nonlinear analysis of out-of-phase oscillations in boiling water reactors. *Ann. Nucl. Energy* 23 (16), 1301.
- Muñoz-Cobo, J.L., Rosello, O., Miró, R., Escrivá, A., Ginestar, D., Verdú, G., 2000. Coupling of density wave oscillations in parallel channels with high order modal kinetics: application to BWR out-of-phase oscillations. *Ann. Nucl. Energy* 27, 1345.
- Rizwan-uddin, 2000. Sub- and supercritical bifurcation and turning points in a simple BWR model. In: *Proc. Int. Top. Mtg. on Advances in Reactor Physics and Mathematics (PHYSOR-2000)*, Pittsburgh, May 7–11, 2000.
- Rizwan-uddin, Dorning, J.J., 1985. Linear and nonlinear stability analyses of density wave oscillation using the drift flux model. In: *ANS Proceedings of the 23rd ASME/AICHe/ANS National Heat Transfer Conference*, Am. Nucl. Soc., LaGrange Park, IL, p. 48.
- Rizwan-uddin, Dorning, J.J., 1986. Some nonlinear dynamics of a heated channel. *Nucl. Eng. Des.* 93, 1.
- Saha, P., Zuber, N., 1978. An analytical study of the thermally induced two-phase flow instabilities including the effect of thermal non-equilibrium. *Int. J. Heat Mass Transfer* 21, 415.
- Saha, P., Ishii, M., Zuber, N., 1976. An experimental investigation of thermally induced flow oscillations in two-phase systems. *J. Heat Transfer* 98, 616.

- Tsuji, M., Nishio, K., Narita, M., 1993. Stability analysis of BWRs using bifurcation theory. *J. Nucl. Sci. Tech.* 30 (11), 1107.
- van Bragt, D.D.B., Rizwan-uddin, van der Hagen, T.H.J.J., 1999. Nonlinear analysis of a natural circulation boiling water reactor. *Nucl. Sci. Eng.* 131, 23.
- Wulf, W., Chen, H.S., Diamond, D.J., Khatib-Rahbar, M., 1984. A description and assessment of RAMONA-3B MOD 0 Cycle 4: A Computer Code with Three Dimensional Neutron Kinetics for BWR System transients. NUREG/CR-3664, 1984.
- Zhou, Quan, Rizwan-uddin, 2002. Bifurcation analyses of in-phase and out-of-phase oscillations in BWRs. In: *Proc. of International Conference on the New Frontiers of Nuclear Technology, Reactor Physics, Safety and High Performance Computing (PHYSOR-2002)*, Seoul, Korea, October 7–10, CD-ROM (2002).